Determination of the cation site distribution of the spinel in multiferroic CoFe2O4 / BaTiO3 layers by X-ray photoelectron spectroscopy

T. Aghavnian, J.B Moussy, D. Stanescu, Rachid Belkhou, N Jedrecy, H. Magnan., P. Ohresser, Arrio M.-A., Ph. Sainctavit, Antoine Barbier

Journal of Electron Spectroscopy and Related Phenomena 202 (2015) 16–21

Contents lists available at ScienceDirect

Journal of Electron Spectroscopy and Related Phenomena

journal homepage: www.elsevier.com/locate/elspec

Determination of the cation site distribution of the spinel in multiferroic $CoFe_2O_4/BaTiO_3$ layers by X-ray photoelectron spectroscopy

T. Aghavnian[a,b], J.-B. Moussy[a], D. Stanescu[a], R. Belkhou[b], N. Jedrecy[c], H. Magnan[a], P. Ohresser[b], M.-A. Arrio[d], Ph. Sainctavit[d], A. Barbier[a,*]

[a] CEA/Saclay, DSM/IRAMIS/SPEC, CNRS UMR 3680, F-91191 Gif-sur-Yvette, France
[b] Synchrotron SOLEIL, L'Orme des Merisiers Saint-Aubin, F-91192 Gif-sur-Yvette, France
[c] Sorbonne Universités, UPMC Univ Paris 06, UMR 7588, INSP, F-75005 Paris, France
[d] IMPMC, F-75015 Paris, France

ARTICLE INFO

Article history:
Received 24 October 2014
Received in revised form 3 February 2015
Accepted 7 February 2015
Available online 16 February 2015

Keywords:
Oxides
Ferrites
Cation distribution
X-ray photoelectron spectroscopy (XPS)
X-ray magnetic circular dichroism (XMCD)

ABSTRACT

The properties of $CoFe_2O_4/BaTiO_3$ artificial multiferroic multilayers strongly depend on the crystalline structure, the stoichiometry and the cation distribution between octahedral (*Oh*) and tetrahedral (*Td*) sites (inversion factor). In the present study, we have investigated epitaxial $CoFe_2O_4$ layers grown on $BaTiO_3$, with different Co/Fe ratios. We determined the cation distribution in our samples by X-ray magnetic circular dichroism (XMCD), a well accepted method to do so, and by X-ray photoelectron spectroscopy (XPS), using a fitting method based on physical considerations. We observed that our XPS approach converged on results consistent with XMCD measurements made on the same samples. Thus, within a careful decomposition based on individual chemical environments it is shown that XPS is fully able to determine the actual inversion factor.

1. Introduction

The ferroelectric perovskite $BaTiO_3$ coupled with the ferrimagnetic spinel $CoFe_2O_4$ is a well referenced system for the study of the magnetic states upon multiferroic couplings [1,2]. Such a study requires to fully analyze the magnetic properties of the spinel of such systems, among them the spinel inversion factor.

We already know that bulk $CoFe_2O_4$ has several key properties such as strong magneto-crystalline anisotropy, high magnetostriction and saturation magnetization, as well as high coercive fields at room temperature [3,4]. Bulk $CoFe_2O_4$ crystallizes in the spinel structure with a lattice parameter of 0.838 nm. The minimal cubic unit cell (i.e. gathering the 4 rhombohedral unit cells imposed by the fcc lattice) contains 8 formula units and the spinel space group is $Fd\bar{3}m$. The Co and Fe cations can occupy either tetrahedral *Td* or octahedral *Oh* sites of the oxygen sublattice. Their distribution follows the formula $[Fe_yCo_{1-y}]_{Td}[Fe_{2-y}Co_y]_{Oh}O_4$, with the spinel inversion parameter y being 0 for a normal spinel and 1 for an inverse one. Lattice energy calculations [5] show that Co^{2+} ions favor *Oh* sites in $CoFe_2O_4$, thus an inverse spinel structure is predicted. In practice y is usually smaller than 1, especially in thin films [6].

To the bests of our knowledge, a precise analysis of the cation distribution inside the spinel of $BaTiO_3$–$CoFe_2O_4$ epitaxial thin layers multiferroics has not been looked into by most of the main references on the subject of magneto-electric coupling [2,7,8]. However, the distribution of those cations within the spinel structure strongly affects the electric and magnetic properties of the samples. For instance, the resulting magnetic moment will be different depending on the cation distribution (an illustration of the concept is detailed for $MnFe_2O_4$ ferrite in Ref. [9]).

It is therefore of high importance to determine this ion site distribution in order to deduce the global magnetic moment, as well as for any magnetic characterization, and in particular in the context of magnetoelectric coupling. X-ray magnetic circular dichroism (XMCD) is considered the most precise technique to determine the inversion parameter; however it requires access to a synchrotron beamline. Alternatively, authors often choose to estimate the cation distribution using X-ray photoelectron spectroscopy (XPS), as it is a common apparatus for spectroscopy in laboratories, and since it is obvious that the spectra have to contain all necessary information like in the X-ray absorption spectroscopy (XAS) case. Nevertheless,

* Corresponding author.
E-mail address: abarbier@cea.fr (A. Barbier).

http://dx.doi.org/10.1016/j.elspec.2015.02.006
0368-2048/

from previous reports no clear and reliable strategy for the XPS fitting procedure was established. It is still unclear how to correctly exploit XPS spectra to extract that data, especially considering that a given fitting method tends to have a non-negligible influence on the result, and methods seem to vary from paper to paper [10,11], sometimes leading to controversies [12,13]. The lack of direct comparison with XMCD does not allow to conclude on the pertinence of the proposed approaches.

Our aim is to define a reliable strategy for XPS data processing based on physical considerations and consistent with XMCD measurements, in order to extract the adequate cation distribution in $CoFe_2O_4$ thin films. For that purpose, we use well-defined epitaxial thin films of $CoFe_2O_4$ (0 0 1) grown on $BaTiO_3$ underlayers. The choice of analyzing spinel samples with different Co/Fe ratios was adopted to insure the stability of the method for a series of samples for which the cation organization is likely to vary. We expect that the present method can be extended to a large variety of other spinels.

Maghemite is the oxidized form of magnetite where all the divalent iron have been replaced by trivalent ones. Indeed three Fe(II) ions can be replaced by two Fe(III) ions and a vacancy. Magnemitization of spinel is observed when part of Fe(II) ions are replaced by Fe(III). By convention, we discuss the degree of spinel inversion independently of the degree of maghemitization, which becomes an additional parameter when Co/Fe differs from 0.5. In the same manner, we define the cationic stoichiometry as the Co/Fe ratio regardless of the divalent/trivalent distribution.

2. Experimental

Three samples of $CoFe_2O_4/BaTiO_3/SrTiO_3$ (0 0 1) were prepared by Atomic-Oxygen assisted Molecular Beam Epitaxy (AO-MBE) [14–16].

The growth was performed in a dedicated AO-MBE setup working in the 10^{-10} mbar pressure range equipped with a radio-frequency plasma source, an Auger electron spectroscopy (AES) analyzer, a reflection high energy electron diffraction (RHEED) gun and connected in ultra high vacuum conditions to a separate ultra-high vacuum chamber with an X-ray photoelectron spectroscopy apparatus. During growth, the samples rotate continuously around the surface normal to obtain homogenous films.

The main features of the samples at different stages of their growth are detailed in Table 1. They mainly differ by having different Co/Fe ratios. Two of the $SrTiO_3$ (0 0 1) substrates were 1% Nb doped (for samples number 1 and 2), the last was undoped (sample 3). All three substrates were annealed in air at 900 °C for 3 h a few weeks before deposition in order to restore the nominal stoichiometry and get rid of the polishing induced defects. We first performed the epitaxial growth of $BaTiO_3$ (0 0 1) on $SrTiO_3$ (0 0 1) in the conditions detailed in [14]. Ba and Ti were deposited from individual Knudsen cells. The growth process was monitored in real time by RHEED, which is a technique that permits to control the crystal quality. The stoichiometry of the samples was checked by AES and XPS after the growth.

Table 1
Main characteristics of the $CoFe_2O_4/BaTiO_3/SrTiO_3$ samples.

Sample	1	2	3
$BaTiO_3$ thickness (nm)	15	13	11
$CoFe_2O_4$ thickness (nm)	6	6	6
XPS Co/Fe	0.28	0.48	0.63
Spinel inversion parameter y_{XMCD}	0.90	0.80	0.90
Spinel inversion parameter y_{XPS}	0.808	0.806	0.824
% $Fe^{3+}{}_{Oh}$ by XMCD	55%	60%	55%
% $Fe^{3+}{}_{Oh}$ by XPS	59.6%	59.7%	58.8%

After the $BaTiO_3$ (0 0 1) crystalline growth the samples were extracted from the AO-MBE chamber and mounted on a different sample holder optimized for $CoFe_2O_4$ growth, then later re-introduced in the same epitaxy chamber. The carbon observed by AES on the $BaTiO_3$, due to air-exposure, was removed by 45 min high brilliance oxygen plasma exposure. Then the ferrite growth was performed as in Ref. [15], and at a temperature of 450 °C. Then again, real time RHEED and post-growth in situ AES and XPS techniques were used.

The XPS apparatus uses twin anodes with a XR3 X-ray source and the hemispherical analyser Alpha110 from society Thermo Electron Corporation. XPS spectra were obtained by using Al-Kα (1486.6 eV) and Mg-Kα (1253.6 eV) X-ray sources. The precaution of using two sources is to insure that the Auger or photoemission peaks cannot be confused. A wide scan of the samples was first realized (0–1200 eV) to detect all the species in the sample. Then we focus on Fe2p, Co 2p and O1s. Those specific energy intervals were then scanned multiple times – typically 10 scans for Co and Fe, 5 for O – in order to maximize the signal to noise ratio. The energy resolution of the XPS spectra is typically around 0.1 eV. Analysis was performed using the software "Avantage Data Spectrum Processing"TM.

The XMCD measurements were performed on DEIMOS (Dichroism Experimental Installation for Magneto-Optical Spectroscopy) beamline at synchrotron SOLEIL (Saint-Aubin, France). DEIMOS is a beam-line dedicated to the study of the magnetic and electronic properties using polarized light. The main advantage of XMCD over other techniques to investigate magnetic behavior is its chemical and orbital selectivity. The energy range is 350–2500 eV, which allows the study of $L_{2,3}$ edges of Fe and Co and the K edge of O. The energy resolution is $E/\Delta E$ from 6000 to 10,000. The overall properties of the beamline [17] give us very clear spectra despite the small thickness of the thin film of spinel of 6 nm. Measurements were performed at 4 K. The cryo-magnet delivers $\pm$7 T along the beam direction and $\pm$2 T perpendicular to the beam. All our XMCD measurements we carried out at 4 K, with an incidence angle of 30° with respect to the surface and a magnetic field of 5 T along the beam direction.

3. Results

The RHEED patterns were recorded during the deposition of both $BaTiO_3$ and $CoFe_2O_4$. An example of final RHEED patterns is reported in Fig. 1. It indicates that the samples are epitaxial and single crystalline. Also, we can observe from the comparison of sample 3 (non-stoichiometric, Co/Fe = 0.63) with a reference stoichiometric sample (Co/Fe = 0.50) that the RHEED patterns are similar. Moderate stoichiometry changes do not seem to affect the observations made using the RHEED technique. X-ray reflectivity measurements performed at 8 keV gave us an average deposition rate of 0.06 nm/min for $BaTiO_3$ and of 0.13 nm/min for $CoFe_2O_4$. The deduced thicknesses of deposition are given in Table 1.

Because our aim is to determine the cation distribution between octahedral and tetrahedral sites in the spinel using XPS, it is necessary to have a reliable and well accepted benchmark. Thus this distribution was first determined using XMCD measurements on DEIMOS beamline. The measurements were performed at the L_3 edge of Fe around 716.7 eV. The experimental plots are presented in Fig. 2, left, for the different samples. The similar form of the XMCD plots indicates that the average electronic structure for Fe is similar for the three samples. In addition, one notices that the samples are inverse spinel. Those plots were fitted using a linear combination of the theoretical [16,18] spectra of Fe^{3+} in octahedral and tetrahedral sites and of Fe^{2+} in octahedral sites (Fig. 2, middle), as these three components are sufficient since Fe^{2+} is not found in tetrahedral sites [16]. The calculated Fe $L_{2,3}$ theoretical

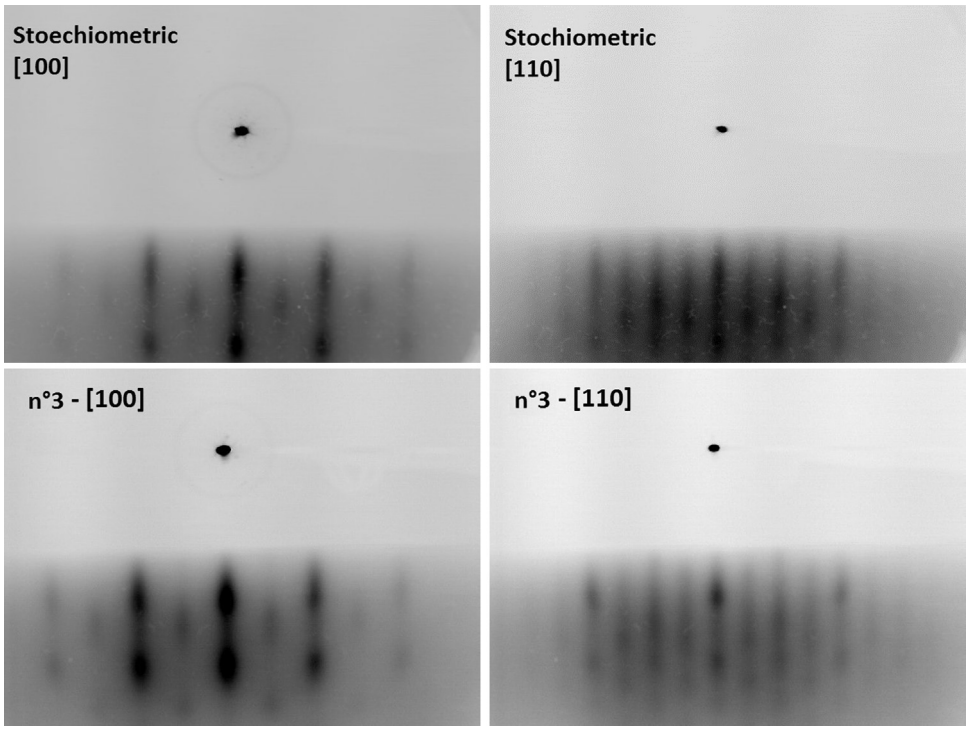

Fig. 1. RHEED patterns after the deposition of $CoFe_2O_4$ on $BaTiO_3$ – stoichiometric sample (top), sample 3 (bottom), [1 0 0] direction (left), [1 1 0] direction (right).

absorption spectra taken from [19,16] originate from a crystal field atomic multiplet approach, taking into account the occupied 3d electron configurations, the crystal field, the spin–orbit coupling and electron–electron interactions within Fe, and the hybridization of 3d electrons to other valence electrons.

The least squares method was applied using two parameters, the Fe^{3+} proportion on the total of Fe^{2+} and Fe^{3+} cations (close to 1 as Fe^{2+} appeared neglectful), and the Fe^{3+} *Oh* proportion on the total of sites Fe^{3+} *Oh* and Fe^{3+} *Td*. This method was used to conclude on the best fitting values (Fig. 2, right).

The percentage of Fe^{3+} in octahedral sites is respectively of 55%, 60% and 55% for samples number 1, 2 and 3. We thus conclude that the $CoFe_2O_4$ thin layers grown on $BaTiO_3$ crystallize mainly in the inverse spinel structure.

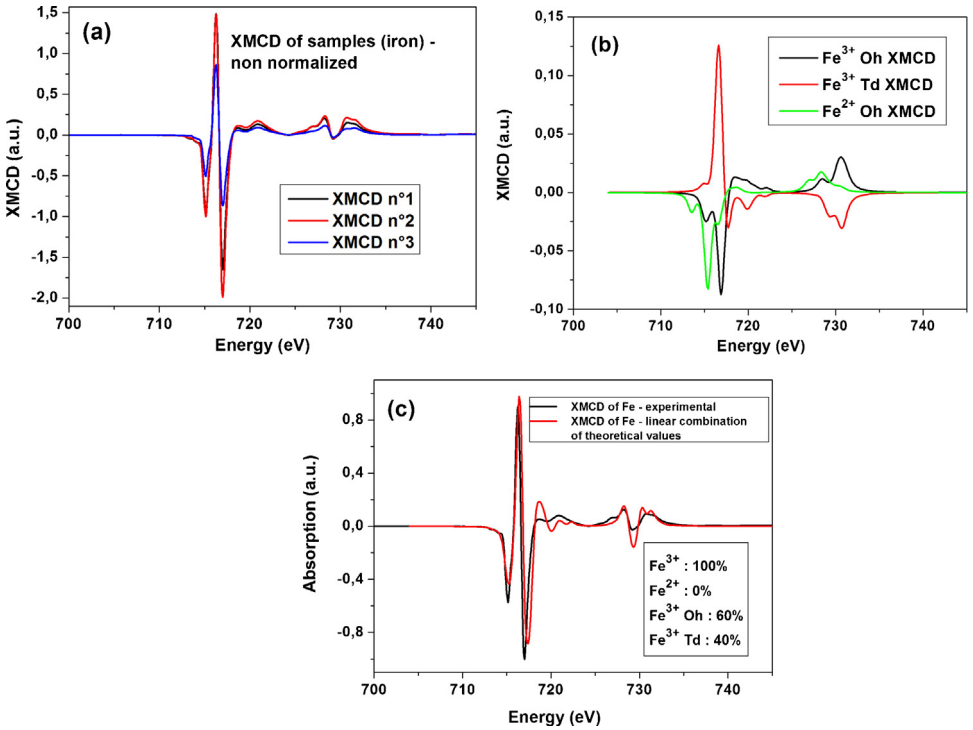

Fig. 2. Experimental XMCD spectra at the $L_{2,3}$ edge of Fe in the samples (a); theoretical XMCD plots of Fe^{3+} *Oh*, Fe^{3+} *Td* and Fe^{2+} *Oh* (b); from Ref. [19], fitted XMCD spectra of the sample 2 recorded at the $L_{2,3}$ edge of Fe, obtained by the least-squared combinatory method (c).

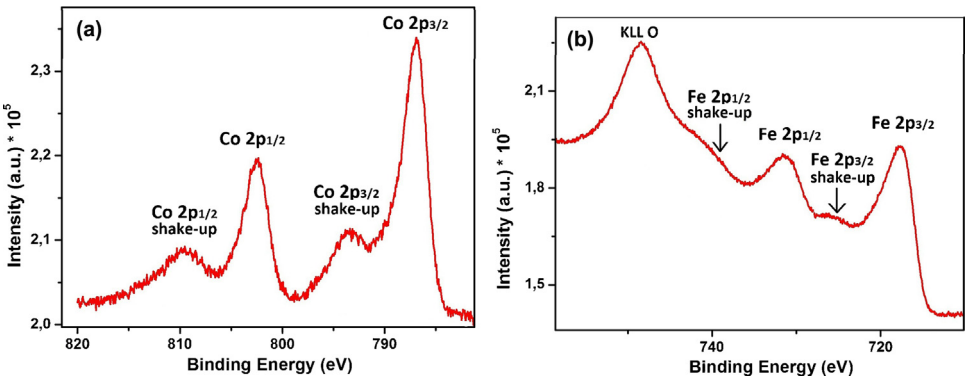

Fig. 3. XPS spectrum of Co in $CoFe_2O_4$ for sample 3 (a). XPS spectrum of Fe in $CoFe_2O_4$ for sample 3 (b).

The XPS spectra that we measured for Co and Fe are presented in Fig. 3. The main components are the peaks corresponding to electronic levels $2p_{3/2}$ and $2p_{1/2}$ and the associated shake-up satellites for both metals. The shake-up peaks are attributed to the transition of an electron from a 3d orbital to the empty 4s orbital during the ejection of the core 2p photoelectron [20].

If the obtained spectra can be similar for different laboratories, the exploitation method tends to vary from paper to paper in literature. Zhou et al. [10] fit XPS spectra on bulk and powder $CoFe_2O_4$ and differentiates *Td* and *Oh* sites, but do not use the same background as us for iron nor fit shake-up satellites. Wang et al. [11] fit also Co and Fe with two peaks, and add the fitting of the shake-up satellite, but only consider the $2p_{3/2}$ ion levels and not the $2p_{1/2}$ as well. The following paragraphs detail our approach towards the exploitation of those XPS spectra.

First of all, beyond the question of site occupation, the XPS spectra allow us also to estimate the stoichiometry of the samples. This was done using a Shirley-type background by fitting the $Co2p_{3/2}$ and $Fe2p_{3/2}$ peaks (octahedral sites and tetrahedral sites and shake-up) and deducing their area. Lets notice that this decomposition has more validity than trying to highlight a separation between different oxidation states of iron as XMCD measurements have shown that Fe^{2+} is less than 1% of Fe^{3+}. This area is then corrected using the corresponding Scofield factors [21]. We chose to estimate the Co/Fe ratio by calculating the one between the Scofield-corrected intensity area of $Co2p_{3/2}$ and $Fe2p_{3/2}$. The choice of $2p_{3/2}$ over $2p_{1/2}$ was because of the higher intensity of signal giving us more precision. This ratio is found to be respectively of 0.28, 0.48 and 0.63 (Table 1) for samples 1, 2 and 3.

Experimentally, it is easier to discriminate the different contributions to the peaks for the Co spectra than for the Fe spectra. This observation was mostly confirmed during the fitting process with the "Avantage Data Spectrum Processing"™ software, which was more reproducible for Co. The main $Co2p_{3/2}$ peak was decomposed into two different peaks ($Co2p_{3/2}$ *Oh* and $Co2p_{3/2}$ *Td* (Fig. 4)) however the main $Fe2p_{3/2}$ peak was too broad and did not allow an obvious discrimination of individual components ($Fe2p_{3/2}$ *Oh* and $Fe2p_{3/2}$ *Td*) by this fit technique. As a consequence, we chose the XPS spectra for Co as a reference for estimating the spinel inversion parameter, rather than Fe. This decomposition in *Oh* and *Td* peaks is common on Fe [22], and we proceeded by analogy to do the same on Co.

We search a methodology allowing to fit the Co2p XPS spectrum in a reproducible way based on physical properties in terms of electronic structure in order to quantitatively assess the ratios of *Oh* and *Td* sites. This method is based upon the following constraints. First of all, we use a Shirley background that covers all the energy range from $Co2p_{3/2}$ to $Co2p_{1/2}$. As a guard rule, for all fits of all elements, we used a Shirley background. The next step is to impose an identical spinel inversion parameter for the $Co2p_{3/2}$ and $Co2p_{1/2}$ states, which implies that the ratio between the areas of the XPS peaks of Co in *Td* and *Oh* sites, Co-Td/Co-Oh, must be the same for both $Co2p_{3/2}$ and $Co2p_{1/2}$. This constraint is relaxed at the end of the fit and the fit is accepted if there is no more than 2% shift from a central value. The third constraint derives from the rigid band approximation [23] linked to the continuity in the perceived environment for the different sites. It implies to keep, for the decomposition of $Co2p_{3/2}$ and $Co2p_{1/2}$ in peaks associated to *Oh* and *Td* sites, the energy gap between both sites $E_{Co-Oh}-E_{Co-Td}$ constant for each electronic configuration. This constraint is relaxed at the end of the fit and the fit is accepted if there is no more than 0.1 eV shift from a central value. The shake-up is a broad peak consisting of a mix of different peaks, and is considered as well represented by a unique peak. We fix no constraints on its energy positioning for the same reasons.

The fit is performed using symmetric peaks in order to limit the number of fitting parameters, even if we cannot exclude some asymmetry. However this method is suitable to give us the relative area of octahedral and tetrahedral peaks which makes a physical sense.

And indeed all these constraints put together give us a unique and perfectly reproducible fit for the Co2p spectra (Table 2). Whatever the initial position before the process, the fit always converges on the same values. This fully justifies to take Co as a reference. However, if we use the same fitting procedure for fitting the Fe2p lines, we observed that the results are strongly dependent of the initial parameter. It is maybe due to larger peaks and presence of different components (Fe^{2+} and Fe^{3+}). Moreover, in the same energy range, there is also the KLL Auger of oxygen (Figs. 3 and 5) which is mixed with the shake-up of $Fe2p_{1/2}$.

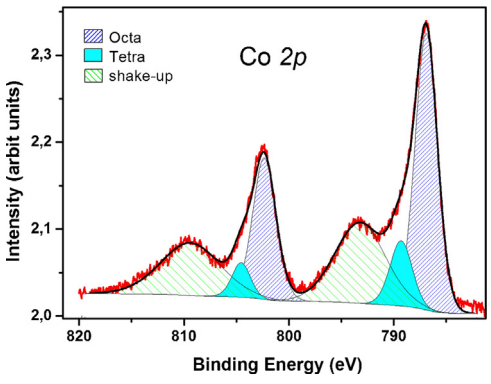

Fig. 4. XPS spectrum of Co in $CoFe_2O_4$, with the best fit peaks for sample 3.

Table 2
Binding energy position of the fitting peaks in XPS for sample 3.

Sample 3	Co	Fe
$2p_{3/2}$ *Oh*	786.95 eV	717.50 eV
$2p_{3/2}$ *Td*	789.35 eV	720.15 eV
$2p_{3/2}$ shake-up	793.35 eV	725.65 eV
$2p_{1/2}$ *Oh*	802.35 eV	731.65 eV
$2p_{1/2}$ *Td*	804.6 eV	733.05 eV
$2p_{1/2}$ shake-up	809.5 eV	740.6 eV

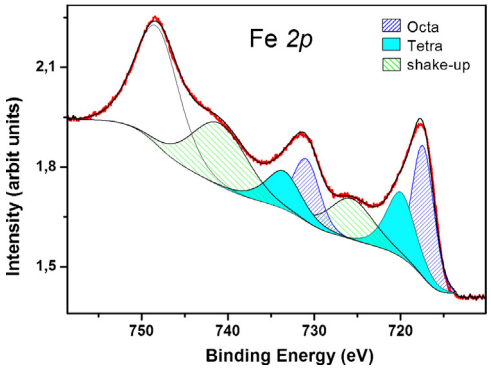

Fig. 5. XPS spectrum of Fe in $CoFe_2O_4$ – decomposition in individual contributions of the best fit for sample 3.

Because an inverse spinel has 100% of its Co in *Oh* sites ($y = 1$), and a normal spinel 100% in *Td* sites ($y = 0$), we deduce the spinel inversion parameter (y) to be equal to the occupation percentage of the cobalt octahedral sites. From the fit of Co 2p spectra, this percentage was found to be, for samples number 1, 2 and 3, of 80.8%, 80.6% and 82.4% respectively. Those results are within a 2% error margin linked to the shift after releasing constraints.

We tried to fit the Fe2p XPS spectra in the same manner, but the reproducibility was a problem. Indeed, we obtained good fits corresponding to significantly different inversion ratios. As a consequence, those spectra could not be used as the reference for our XPS method. However, as we examine the same sample, it is possible to impose the supplementary constraint of having the same spinel inversion parameter as determined from the Co2p spectrum. Using this added constraint, we can find a good fit that corresponds to the expected results, and which is moreover unique (Fig. 5 and Table 2).

Concerning the Fe2p fitting, we found that it is important to determine the background over a large range including the huge peak at ≈748 eV corresponding to the KLL Auger peak of oxygen, which contributes massively to the background. It is here a better solution than switching to an Al Kα source to eliminate the Auger contribution of O, as the Auger contribution of Co would then overlap in energy with Fe2p.

4. Discussion

The difference of binding energy between octahedral and tetrahedral sites for samples number 1, 2 and 3 are respectively of 2.75 eV, 2.23 eV and 2.63 eV for Fe2p (average values of $Fe2p_{3/2}$ and $Fe2p_{1/2}$), within a 0.1 eV margin, and of 2.40 eV, 2.35 eV and 2.38 eV for Co 2p. These values are close to the one found for $CoFe_2O_4$ nanoparticles [10] (3 eV for Fe2p and 2.10 eV for Co2p), where the amount of normal spinel structure is higher than in our samples. Comparing our results with other experiments on similar samples can give discrepancies [24] since some do not take into account the Co $2p_{1/2}$ peak or have not fitted the shake-up satellite. It so seems that taking into account all parameters – background, electronic levels $2p_{3/2}$ and $2p_{1/2}$, shake-up satellites – is key in finding a unified method of XPS analysis.

The fact that the difference in binding energy between octahedral site and tetrahedral site in XPS is bigger that the difference of absorption edges of the same sites is not really surprising. Indeed, the screening of the core hole is reflected in the spectra in a completely different manner for the two processes.

The inversion parameter y obtained using the XPS method, of 80.8%, 80.6% and 82.4% for samples number 1, 2 and 3, can be linked to the estimated percentage of Fe^{3+} in octahedral and tetrahedral sites. If we consider that in an inverse spinel, Fe^{3+} is in similar proportion in both *Oh* and *Td* sites, and that in a normal spinel all Fe^{3+} are in *Oh* sites, we find that $\%Fe(Oh) = (y \times 0.5 + (1-y) \times 1) \times 100$ which is 59.6%, 59.7% and 58.8%. Each of those results is less than 5% different from results from XMCD – 55%, 60% and 55% for samples number 1, 2 and 3 – which is in the error margin of the XPS technique.

We can also observe that the spinel inversion parameter y seems fairly independent of the Co/Fe ratio, so of the stoichiometry of the spinel. This result is quite surprising [25]. Indeed, for stoichiometries with low Co^{2+} cations content, we would have expected iron cations to replace some of the *Oh* sites, modifying thus the inversion parameter. Or a maghemitization of the crystal, which would mean cationic vacancies but would imply also a small change of the inversion parameter.

The results indicate that the spinel of our $BaTiO_3$–$CoFe_2O_4$ multiferroic thin layers crystallizes in a mostly inverse configuration and thus of high magnetic moment.

If XMCD remains a recognized method when looking for a precise determination of the spinel inversion parameter y, we show that XPS spectra coupled to physical constraints for the analysis, can give a complementary estimation. Both XMCD and XPS methods yield very similar results. This convinces us that XPS can be an excellent synchrotron free approach, when a 5% error on the sought information remains an acceptable precision.

5. Conclusion

We have grown $CoFe_2O_4/BaTiO_3/SrTiO_3$ samples by oxygen-assisted molecular beam epitaxy, fully controlled in crystalline structure and stoichiometry. The spinel film of $CoFe_2O_4$ was studied both in XMCD and XPS. To perform that study, we focused on the Fe spectra in XMCD and the Co spectra in XPS. To fit correctly the Fe spectra in XPS, it appeared necessary to perform the scan on a large band of energy around Fe to obtain the actual background. Using physical considerations to impose constraints to the fit of the XPS spectra, we managed to obtain quantitative values of the distribution of the Co and Fe cations between octahedral and tetrahedral sites of the spinel. Those values were fully consistent with the XMCD results obtained on the same samples, therefore confirming our approach. We also highlighted the inverse nature of the spinel. This method can be of major utility to obtain routinely those values in laboratories equipped with an XPS apparatus, rather than having to perform the determination on a synchrotron beamline. It is also likely applicable to any other spinel ferrites such as $CrFe_2O_4$, $MnFe_2O_4$, $NiFe_2O_4$, $CuFe_2O_4$.

Acknowledgements

We acknowledge SOLEIL for provision of synchrotron radiation facilities and are grateful to the SOLEIL-DEIMOS beamline staff members who helped achieve those experiments. This work was partly supported by the CNano-MAEBA grant, for which we are also grateful.

References

[1] R. Chopdekar, V. Malik, A.F. Rodríguez, L. Le Guyader, Y. Takamura, A. Scholl, D. Stender, C. Schneider, C. Bernhard, F. Nolting, et al., Phys. Rev. B 86 (2012) 014408.
[2] H. Zheng, J. Wang, S. Lofland, Z. Ma, L. Mohaddes-Ardabili, T. Zhao, L. Salamanca-Riba, S. Shinde, S. Ogale, F. Bai, et al., Science 303 (2004) 661.
[3] J. Ryu, A.V. Carazo, K. Uchino, H.-E. Kim, Jpn. J. Appl. Phys. 40 (2001) 4948.
[4] E. Manova, B. Kunev, D. Paneva, I. Mitov, L. Petrov, C. Estournes, C. D'Orléan, J.-L. Rehspringer, M. Kurmoo, Chem. Mater. 16 (2004) 5689.
[5] H.S.C. O'Neill, A. Navrotsky, Am. Mineral. 68 (1983) 181.
[6] S. Matzen, Films ultraminces épitaxiés de $MnFe_2O_4$, $CoFe_2O_4$ et $NiFe_2O_4$ pour le filtrage de spin à température ambiante, Université Pierre et Marie Curie - Paris VI, 2011 (Ph.D. thesis).
[7] C.A. Vaz, J. Hoffman, C.H. Ahn, R. Ramesh, Adv. Mater. 22 (2010) 2900.
[8] R. Chopdekar, Y. Suzuki, Appl. Phys. Lett. 89 (2006) 182506.
[9] S. Matzen, J.-B. Moussy, R. Mattana, K. Bouzehouane, C. Deranlot, F. Petroff, J. Cezar, M.-A. Arrio, P. Sainctavit, C. Gatel, et al., Phys. Rev. B 83 (2011) 184402.
[10] Z. Zhou, Y. Zhang, Z. Wang, W. Wei, W. Tang, J. Shi, R. Xiong, Appl. Surf. Sci. 254 (2008) 6972.
[11] W.P. Wang, H. Yang, T. Xian, J.L. Jiang, Mater. Trans. 53 (2012) 1586.
[12] E. Paparazzo, J. Electron Spectrosc. Relat. Phenom. 154 (2006) 38.
[13] T. Yamashita, P. Hayes, J. Electron Spectrosc. Relat. Phenom. 154 (2006) 41.
[14] A. Barbier, C. Mocuta, D. Stanescu, P. Jegou, N. Jedrecy, H. Magnan, J. Appl. Phys. 112 (2012) 114116.
[15] A. Ramos, J.-B. Moussy, M.-J. Guittet, M. Gautier-Soyer, C. Gatel, P. Bayle-Guillemaud, B. Warot-Fonrose, E. Snoeck, Phys. Rev. B 75 (2007) 224421.
[16] S. Matzen, J.-B. Moussy, R. Mattana, F. Petroff, C. Gatel, B. Warot-Fonrose, J. Cezar, A. Barbier, M.-A. Arrio, P. Sainctavit, Appl. Phys. Lett. 99 (2011) 052514.
[17] P. Ohresser, E. Otero, F. Choueikani, K. Chen, S. Stanescu, F. Deschamps, T. Moreno, F. Polack, B. Lagarde, J.-P. Daguerre, et al., Rev. Sci. Instrum. 85 (2014) 013106.
[18] C. Carvallo, P. Sainctavit, M.-A. Arrio, N. Menguy, Y. Wang, G. Ona-Nguema, S. Brice-Profeta, Am. Mineral. 93 (2008) 880.
[19] P. Kuiper, B. Searle, L.-C. Duda, R. Wolf, P. Van der Zaag, J. Electron Spectrosc. Relat. Phenom. 86 (1997) 107.
[20] L. Yin, I. Adler, T. Tsang, L. Matienzo, S. Grim, Chem. Phys. Lett. 24 (1974) 81.
[21] J. Scofield, J. Electron Spectrosc. Relat. Phenom. 8 (1976) 129.
[22] T. Fujii, F. De Groot, G. Sawatzky, F. Voogt, T. Hibma, K. Okada, Phys. Rev. B 59 (1999) 3195.
[23] D. Spanjaard, C. Guillot, M.-C. Desjonqueres, G. Tréglia, J. Lecante, Surf. Sci. Rep. 5 (1985) 1.
[24] W. Wang, H. Yang, T. Xian, J. Jiang, Mater. Trans. 53 (2012) 1586.
[25] S. Nasrazadani, A. Raman, Corros. Sci. 34 (1993) 1355.